

Supporting information for

DNA-based Nanoparticle Tension Sensors Reveal that T-cell Receptors Transmit Defined pN Forces to Their Antigens for Enhanced Fidelity

Authors: Yang Liu,¹ Lori Blanchfield,² Victor Pui-Yan Ma,¹ Rakieb Andargachew,² Kornelia Galior,¹ Zheng Liu,¹ Brian Evavold,² Khalid Salaita^{1,3*}

Affiliations:

¹Department of Chemistry, Emory University, Atlanta, GA 30322, USA

²Department of Microbiology and Immunology, Emory University School of Medicine, Atlanta, GA 30322, USA

³Wallace H. Coulter Department of Biomedical Engineering, Emory University and Georgia Institute of Technology, Atlanta, GA 30332, USA

* Correspondence to: k.salaita@emory.edu

This PDF file includes:

Materials and methods

Table S1 DNA sequences

Supplementary movie caption

Supplementary note 1 & 2

Fig. S1. Fabrication of DNA-based gold nanoparticle tension sensor surface

Fig. S2. Quenching efficiency calibration of DNA-AuNP tension probes

Fig. S3. Quantification of the average number of DNA sensors per gold nanoparticle

Fig. S4. Tension signals are specifically generated through TCR-ligand interaction

Fig. S5. Investigation of cytoskeletal elements mediating TCR forces

Fig. S6. Colocalization of TCR tension with F-actin, and F-actin with myosin light chain kinase

Fig. S7. Induction of 19 pN sensor by shear flow

Fig. S8. Radial distribution function analysis of TCR tension upon ligand stimulation

Fig. S9. Spatial correlation analysis between TCR tension and active Lck

Fig. S10. Quantification of TCR tension upon perturbation of TCR, CD8 and Lck activities

Fig. S11. Co-presentation of ICAM-1 and DNA tension sensor-pMHC ligands on AuNP

Fig. S12. Comparison of TCR forces and $[Ca^{2+}]$ between V4 and N4 ligand

Fig. S13. Comparison of TGT rupturing between 12 pN and 56 pN probes

Materials and Methods

Reagents

(3-Aminopropyl) trimethoxysilane (97%, APTMS), triethylammonium acetate (TEAA), hank's balanced salts, NiSO₄.6H₂O, Lck inhibitor (7-cyclopentyl-5-(4-phenoxyphenyl)-7H-pyrrolo[2,3-d]pyrimidin-4-ylamine), ROCK inhibitor (Y-27632), MLCK inhibitor (ML-7), F-actin inhibitor (Cytochalasin D), Arp2/3 inhibitor (CK-666), Rac1 inhibitor (NSC23766) were purchased from Sigma-Aldrich (St. Louis, MO) and used without further purification. Cdc42 inhibitor (ML141) was purchased from Santa Cruz Biotech (Dallas, Texas). The fluorescent dye Cy3B-NHS ester was purchased from GE healthcare Bio-Science (Pittsburgh, PA). Number two glass coverslips, ascorbic acid (>99.0%), and 96-well plates were purchased from Fisher Chemical & Scientific (Pittsburgh, PA). DMF (>99.5%), DMSO (99.5%) and sodium bicarbonate (99.0%) were purchased from EMD chemicals (Philadelphia, PA). P2 gel size exclusion beads were acquired from Biorad (Hercules, CA). Lipoic Acid-PEG-NHS (MW 3400) and mPEG-NHS (MW 2000) were purchased from Nanocs (New York, NY). NTA-SAM reagent was purchased from Dojindo (Rockville, Maryland). Recombinant mouse ICAM-1 Fc histag protein (catalog # 83550) was purchased from Biorbyt (San Francisco, CA). AuNPs were custom synthesized and characterized by TEM by Nanocomposix (San Diego, CA). Based on TEM analysis that was provided by the manufacturer, the mean diameter of these particles was 8.6 ± 0.6 nm.

Antibodies

Alexa fluor 647 conjugated anti-TCR antibody (catalog # HM3621) and phalloidin (A22287) was purchased from Life technologies (Grand Island, NY). Anti-Myosin light chain kinase antibody (EP1458Y) was purchased from Abcam (Cambridge, MA). Alexa fluor 647 conjugated anti-Zap70 (pY319) was purchased from BD Bioscience (catalog # 557817). p-Lck (Tyr 394) rabbit polyclonal IgG was purchased from Santa Cruz (catalog # sc-101728). Anti-mouse CD3 epsilon antibody (catalog # 16-0031) was purchased from ebioscience (San Diego, CA). Anti-mouse CD8a blocking antibody (catalog # CL168AP) was purchased from Cedarlane (Burlington, NC). Secondary antibodies, including Alexa fluor 488 goat anti-rat IgG (H+L), Alexa fluor 488 goat anti-rabbit IgG (H+L) and Alexa fluor 647 goat anti-rabbit IgG (H+L), were purchased from Life technologies (Grand Island, NY).

MHC

Biotinylated H-2K(b) monomers were provided by the National Institutes of Health Tetramer Core Facility at Emory University. Monomers are comprised of the designated peptide loaded in the alpha chain of mouse H-2K(b) that is complexed with beta-2-microglobulin (b2m) from either mouse or human origin. In some experiments, the H-2K(b) alpha chain was mutated to prevent the binding of the CD8 co-receptor and these monomers are designated mut to distinguish them from wild type H-2K(b). Specifically, the mouse alpha 3 domain of H-2K(b) was substituted with the alpha 3 domain of human HLA-A2. The peptides folded into the monomers include the cognate chicken ovalbumin 257-264 epitope SIIINFEKL (N4) as well as altered forms of the peptide SIIQFEKL (Q4) and SIIVFEKL (V4); more specifically the monomers are designated wild type mouse b2m N4, mut mouse b2m N4, wild type mouse b2m V4 and mouse or human b2m Q4. As a negative control to show specificity, we used the wild type H-2K(b) with human b2m and the GP33-41 epitope of lymphocytic choriomeningitis virus (LCMV).

OT-1 cell harvesting and purification.

OT-1 T cell receptor transgenic mice were housed and bred in the Division of Animal Resources Facility at Emory University in accordance with the Institutional Animal Care and Use Committee. OT-1 T cells express the CD8 co-receptor and specifically recognize chicken ovalbumin epitope 257–264 (SIINFEKL) in the context of the MHC allele H-2K^b. Naïve OT-1 T cells were enriched from the spleen using magnetic activated cell sorting according to manufacturer instructions provided with the CD8a+ T cell Isolation Kit (Miltenyi Biotec). Briefly, a single cell suspension of splenocytes was obtained and incubated with biotinylated antibodies specific for unwanted splenic cell populations. These populations were separated from the OT-1 T cells following incubation with anti-biotin magnetic beads and enrichment on a magnetic column. Purified T cells were washed in complete RPMI media [1x RPMI 1640 (Corning), 10% heat-inactivated fetal bovine serum albumin, 10 mM HEPES buffer (Corning), 50mg/mL gentamicin solution (Corning), 5 x 10⁻⁵ M 2-mercaptoethanol and 2 mM L-glutamine (Sigma-Aldrich) and analyzed for purity on the same day.

DNA sequences

All DNA strands used were custom synthesized and desalted by Integrated DNA Technologies (Coralville, Iowa), except that quencher strand was synthesized by Biosearch technologies (Petaluma, CA) (Table S1).

Strand ID	DNA Sequences (5' to 3')
A21B	/5AmMC6/ - CGC ATC TGT GCG GTA TTT CAC TTT - /3Bio/
Quencher	/5ThiolMC6-D/ - TTT GCT GGG CTA CGT GGC GCT CTT - /3BHQ_2/
Hairpin (12 pN)	GTG AAA TAC CGC ACA GAT GCG TTT <u>GGG TTA ACA TCT</u> <u>AGA TTC TAT TTT TAG AAT CTA GAT GTT AAC CCT TTA</u> AGA GCG CCA CGT AGC CCA GC
Hairpin (19 pN)	GTG AAA TAC CGC ACA GAT GCG TTT <u>CGC CGC GGG CCG</u> <u>GCG CGC GGT TTT CCG CGC GCC GGC CCG CGG CGT TTA</u> AGA GCG CCA CGT AGC CCA GC
Scrambled hairpin	GTG AAA TAC CGC ACA GAT GCG TTT <u>ATC GTC AAT ATA</u> <u>TAC GAT ATT TTT TAG AAT CTA GAT GTT AAC TTT TTA</u> AGA GCG CCA CGT AGC CCA GC
Complement to the scrambled hairpin	AAA AAG TTA ACA TCT AGA TTC TAA AAA ATA TCG TAT ATA TTG ACG ATA AA
TGT thiol anchor strand	/5ThiolMC6-D/TTT TTT TTT TCA CAG CAC GGA GGC ACG ACA C
TGT biotin strand (12 pN)	/5Biosg/GT GTC GTG CCT CCG TGC TGT G
TGT biotin strand (56 pN)	GT GTC GTG CCT CCG TGC TGT G/3Bio/

Table S1. DNA sequences. Underscore indicates the stem-loop forming region within hairpins.

$F_{1/2}$ calculation for 35% GC content hairpin (12 pN). The following $F_{1/2}$ calculation was primarily based on the assumptions and measurements used by Woodside et al. (1) The total free energy of the hairpin can be described as follows:

$$\Delta G(F, x) = \Delta G_{fold} + \Delta G_{stretch} + F \times x \quad (\text{eq. 1})$$

, where ΔG_{fold} is the free energy of unfolding the hairpin at $F = 0$, F is the externally exerted force, x is the hairpin extension and $\Delta G_{stretch}$ is the free energy of stretching the ssDNA from $F = 0$ to $F = F_{1/2}$, and can be calculated from worm-like chain model as follows:

$$\Delta G_{stretch} = \frac{k_B T}{L_p} \frac{L_0}{4 \left(1 - \frac{x}{L_0}\right)} \left[3 \left(\frac{x}{L_0}\right)^2 - 2 \left(\frac{x}{L_0}\right)^3 \right] \quad (\text{eq. 2})$$

where L_p is the persistence length of ssDNA (~ 1.3 nm), L_0 is the contour length of ssDNA (~ 0.63 per nucleotide and ~ 27.7 nm for 44 nucleotides), x is the hairpin extension from equilibrium and was calculated by using $(0.44 - (n-1))$ nm, and k_B is the Boltzmann constant and T is temperature. To use these equations and estimate the $F_{1/2}$ for each hairpin probe, we determined the sum of ΔG_{fold} and $\Delta G_{stretch}$, and estimated the hairpin displacement needed for unfolding, Δx , by using $((0.44 \times (n - 1)) - 2)$ nm, where n represents the number of bases comprising the hairpin. Note that we subtract a distance of 2 nm because this corresponds to the initial separation between the hairpin termini, which is set by the diameter of the hairpin stem duplex (effective helix width). When $F = F_{1/2}$, then the free energy of the transition equals zero and the $F_{1/2}$ can be rearranged as follows:

$$F_{1/2} = \frac{(\Delta G_{fold} + \Delta G_{stretch})}{\Delta x} \quad (\text{eq. 3})$$

In our calculations, $\Delta G_{stretch}$ was determined using equation 2 without modification. ΔG_{fold} was determined using nearest neighbour free energy parameters obtained from the IDT oligoanalyzer 3.1, which uses the UNAFold software package. Eq. 3 was used to infer the $F_{1/2}$ for tension probes at experimental conditions (23 °C, 137.3 mM Na⁺ and 0.8 mM Mg²⁺).

Strand ID	ΔG_{fold} (kJ/mol)	$\Delta G_{stretch}$ (kJ/mol)	Δx (nm)	$F_{1/2}$
Hairpin (12 pN)	90.83	31.69	16.92	12.0

Table S2. $F_{1/2}$ calculation for 12 pN DNA probe

$F_{1/2}$ calculation for 100% GC content hairpin (19 pN) is 19.9 pN. However, this hairpin has been experimentally tested and reported (1, 2). The experimental calibration indicates a $F_{1/2}$ of 19.3 pN. Therefore, we refer to this as the 19 pN hairpin throughout the paper.

Surface Preparation. No.2 glass coverslips were rinsed and sonicated with nanopure water ($18.2 \text{ M } \Omega \text{ cm}^{-1}$) for 30 min, and then sonicated with acetone for 15 min. The cleaned slides were then dried in an oven set at 80 °C for 10 min. Fresh piranha solution (7:3 v/v = H₂SO₄: H₂O₂)

was mixed and then used to clean the substrates for 30 min. Afterwards, the substrates were rinsed with copious amount of nanopure water. The substrates were then sonicated in acetone to remove excess water and to further clean the substrate. Subsequently, 1% v/v APTMS solution in acetone was added to the slides and incubated for 2 h. The amine-modified coverslips were then rinsed in acetone and water and dried under a stream of N₂.

The slides were then annealed for 1 h at 80 °C. The surface was then passivated with 5% w/v mPEG-NHS (MW 2000) and 0.5% w/v lipoic acid-PEG (MW 3400) in 200 µl of 0.1 M fresh sodium bicarbonate solution. After overnight incubation at 4 °C, the excess unreacted PEG molecules were rinsed with nanopure water. This strategy affords a glass surface with sufficient lipoic acid groups to irreversibly anchor AuNP MTFM sensors at appropriate densities. Finally, coverslips were incubated with 20 nM of unmodified 9 nm AuNP solution for 30 min and then rinsed with nanopure water to remove nonspecifically bound particles.

The DNA tension probe hairpins were assembled in 1X PBS by mixing the Cy3B labeled A21B strand (0.33 µM), quencher strand (0.33 µM) and hairpin strand (0.3µM) in the ratio of 1.1: 1.1: 1. The solution was then heated to 95 °C for 5 min by using a heat block and cooled back to room-temperature over a period of 30 min. Afterwards, an additional 2.7 µM of BHQ2 strands were introduced into the DNA assembly solution in 1 M NaCl. 100 µl of this final solution was added between two AuNP functionalized coverslips and incubated overnight at 4 °C.

DNA tension probe modified coverslips were rinsed in 1X PBS before further functionalization with 40 µg/ml of streptavidin in 1X PBS. After 1 h incubation, the coverslips were rinsed in 1 X PBS to remove the unbound streptavidin, which was followed by the final modification with 40 µg/ml of biotinylated ligands (pMHC or α-CD3) in 1X PBS for 1 h. These modified coverslips were then assembled into cell imaging chambers (Attofluor, Life Technologies) filled with hank's balanced salt imaging buffer and immediately used for cell experiments.

In the case of tension gauge tether (TGT), a 75 x 25 mm glass slide was cleaned and functionalized with amine groups using the aforementioned method. A 6 channel µ-Slide was then mounted to the glass slide to create 6 well flow chambers, which was then passivated with 5% w/v mPEG-NHS (MW 2000) and 0.5% w/v lipoic acid-PEG (MW 3400) in 0.1 M fresh sodium bicarbonate solution at 4 °C for overnight. Surfaces were washed extensively with nanopure water and then 20 nM AuNP solution was introduced and incubated for 30 min. After thorough rinsing, the hybridized TGTs were dissolved in 1 M sodium chloride solution and were incubated overnight at 4 °C with 10 µM of HS-(CH₂)₁₁-(OCH₂CH₂)₆-OCH₃ passivating polyethylene glycol. Excess DNA and PEG were removed with three washes of 1X PBS. Afterwards, 40 µg/mL of streptavidin was added and incubated for 1 h. The surfaces were then washed with 1X PBS and subsequently 40 µg/ml of biotinylated ligands (pMHC or α-CD3) was added and allowed to bind to the streptavidin modified duplexes for 1 h. Unbound ligand was washed away with 1X PBS and the surfaces were used within the same day of preparation.

Bulk fluorescence measurement. The fluorescence intensity of Cy3B was recorded using a Biotek Synergy HT plate reader operated using a filter set with excitation/emission $\lambda = 565$ nm/610 nm. Each well in the 96-well plate (Fisher scientific) was filled to a volume of 100 µl.

All measurements were performed in triplicate, and the reported error bars represent the standard deviation of these measurements.

HPLC. Reaction products were purified using a C18 column (diameter: 4.6 mm; length: 250 mm) in a reverse phase binary pump HPLC that was coupled to a diode array detector (Agilent 1100).

MALDI-mass spectrometry. Concentration of the purified oligonucleotide conjugate was determined by measuring its A_{260} value on Nanodrop 2000 UV-Vis Spectrophotometer (Thermo Scientific). MALDI-TOF mass spectrometry was performed on a high performance MALDI time-of-flight mass spectrometer (Voyager STR). The matrix for all experiments was prepared by freshly dissolving excess of 3-hydroxypicolinic acid (3-HPA) in the matrix solvent (50% MeCN/H₂O, 1% TFA, 10% of 50 mg/ml ammonium citrate).

Calcium imaging. Freshly purified OT1 cells ($n = 1 \times 10^6$) were centrifuged to remove the RPMI media and re-suspended in 3 ml of hank's imaging buffer. 10 μ l of 1 mM of fura-2/Am in DMSO was added into the cell suspension. The mixture solution was kept at 37 °C for 30 min. Afterwards, cells were pelleted by centrifugation at 1200 rpm for 4 min and re-suspended in 3 ml of imaging buffer for additional 15 min incubation. This step is to ensure full de-esterification of the fura-2/Am. Then, the cells were again pelleted in previous described condition and re-suspended in 1 ml of imaging buffer and prepared for seeding.

Nikon CFI S Fluor 100x oil objective, a Chroma 340 excitation filter set (ET340x, T400lp and ET510/80m) and Chroma 380 excitation filter set (ET380x, T400lp and ET510/80m) was used to image and quantify the 510 nm fluorescence intensity with excitation at both 340 nm and 380 nm of fura-2 dye. During an experiment, the fluorescence images were acquired by using 340 and 380 filter sets sequentially. Afterwards, ImageJ was used to generate a cell mask for both channels excited by 340 nm and 380 nm. Final fura-2 ratio (I_{340}/I_{380}) was calculated by using the image calculator function in ImageJ.

Fluorescence immunostaining. Naïve OT1 cells were seeded onto the tension probe surfaces decorated with different stimulatory ligands. After cell spreading and activation, 4% of paraformaldehyde was gently added to the imaging chamber for 30 min. After thoroughly rinsing with 1X PBS, 0.1% Triton-X was added to the chamber for 10 min. Subsequently, 1X PBS was used to rinse the chamber, which is followed by 2% w/v BSA passivation for 24 h at 4 °C. Without rinsing, primary antibody was directly added into the chamber for targeting the protein of interests and incubate for 1 h at room temperature. Optionally, fluorescently labeled secondary antibody was also added and incubated for 1 h for visualization when primary antibody was not labeled. The standard manufacture recommended concentrations and conditions were used for immunostaining.

Drug Inhibition. For Lck inhibition, 30 μ M of Lck inhibitor was incubated with OT1 cells either before or after cell plating. In probing cytoskeletal activities, 40 μ M ROCK inhibitor (Y-27632), 40 μ M MLCK inhibitor (ML-7), 20 μ M F-actin inhibitor (Cytochalasin D), 50 μ M Arp2/3 inhibitor (CK-666) was added after 30 min cell plating, respectively. In probing GTPase activities, 200 μ M Rac1 inhibitor (NSC23766) and 10 μ M Cdc42 inhibitor (ML141) was

pretreated with freshly purified OT1 cells ($n = 1 \times 10^6$), respectively, for 30 min before cell plating.

AFM imaging. The density of AuNP tension sensor on the functionalized glass coverslip was measured by using an atomic force microscope mounted on an anti-vibration stage (MFP-3D, Asylum Research, CA). Silicon AFM tips (MikroMasch) with a force constant (5.4-16 N/m) were used to image the sample in tapping mode at a scan rate of 1 Hz. All images were processed and rendered using IgorPro.

Supplementary movie captions

Movie S1. Simultaneous imaging of TCR tension generation and T cell activation

Timelapse video showing a naïve OT1 cell pre-treated with fura-2 ratiometric dye plated on a 19 pN tension probe substrate presenting α -CD3. The video was 10 min long. The RICM channel (left), TCR tension channel (middle) and fura-2 ratio channel (right) are shown side by side.

Movie S2. ML-7 leads to the shrinkage of cell-surface contact and condensation of tension

Timelapse video showing naïve OT1 cells plated on a 12 pN tension probe substrate presenting N4 pMHC upon treatment with 40 μ M of ML7. $t = 0$ min represents the time at which ML7 was added. Brightfield, RICM, TCR tension, and merged channel from RICM and tension are shown from left to right.

Movie S3. TCR tension dynamics in response to pMHC stimulation

Timelapse video of naïve OT1 cells plated on a 12 pN tension probe substrate presenting N4 pMHC. The timelapse movie was captured from $t = 0$ min to $t = 34$ min to show the spatiotemporal dynamics of TCR tension upon cell-substrate contact. RICM, TCR tension, and merged channel from RICM and tension are shown from left to right.

Movie S4. Cell migration and tension dynamics in response to the copresentation of pMHC/ICAM-1

Timelapse video of naïve OT1 cells plated on a 19 pN tension probe substrate co-presenting N4 pMHC and ICAM-1 ligands 15 min after plating. The timelapse movie was captured for 10 min to show the migratory behavior of T cells and characteristic TCR tension at the trailing edge. The interval between each frame is 30 s. Brightfield (top left), RICM (top right), TCR tension (bottom left), and merged channel from RICM and tension (bottom right) are shown in a quadrant.

Movie S5. OT-1 Cell tension dynamics and $[Ca^{2+}]$ flux in response to the V4 ligand

Timelapse video of naïve OT1 cells pre-treated with fura-2 ratiometric dye plated on 12 pN tension probe substrate presenting V4 pMHC. The timelapse movie was \sim 10 min long. The RICM channel (left), TCR tension channel (middle) and fura-2 ratio channel (right) are shown side by side. Normalized fura-2 ratio was colored coded representing the value from 1.0 to 2.0.

Movie S6. OT-1 Cell tension dynamics and $[Ca^{2+}]$ flux in response to the N4 ligand

Timelapse video of naïve OT1 cells pre-treated with fura-2 ratiometric dye plated on 12 pN tension probe substrate presenting N4 pMHC. The timelapse movie was \sim 6 min long. The RICM channel (left), TCR tension channel (middle) and fura-2 ratio channel (right) are shown side by side. Normalized fura-2 ratio was colored coded representing the value from 1.0 to 5.0.

Supplementary Note 1

The DNA-based nanoparticle tension probes displayed a 103-fold increase in fluorescence increase upon unfolding (Fig. 1B). Based on AFM analysis, the density of gold nanoparticles sensors is approximately 11 AuNPs per EMCCD pixel area (160 nm × 160 nm). Bulk fluorescence measurements indicate that an average of 4.4 DNA hairpins are bound per AuNP. Given that the maximum fluorescence signal associated with the fully opened hairpin sensors is 37900 a.u. per pixel, we estimate that each activated tension sensor contributes a value of 783 a.u. in fluorescence. This analysis indicates that a minimum of ~31 DNA hairpins ($F_{1/2} = 19$ pN) are mechanically unfolded per μm^2 based on the αCD3 stimulation data shown in Fig. 2E. Note that only a subset of bound TCR molecules transmit mechanical forces sufficient to unfold the DNA hairpins. In principle, these AuNP-DNA based tension probes provide sufficient sensitivity for single molecule detection.

Supplementary Note 2

All the DNA tension probes used in this study are either experimentally calibrated (19 pN) using single molecule spectroscopy methods (1, 2) or theoretically calculated based on literature precedent for the $F_{1/2} = 12$ pN at 23 °C (see Table S2 in SI methods). Therefore, T cell experiments were performed at the room temperature rather than 37 °C. We acknowledge that this temperature choice may lead to suboptimal cell activity such as delayed calcium flux. Nonetheless, we observed significant phosphorylation of Lck and Zap70 within a few minutes following cell seeding (Fig. 2C), which is in agreement with the rates of T cell activation in other reported work (3). This suggests that T cell response is not compromised in our experimental conditions.

In experiments using TGTs to physically limit the maximum TCR-pMHC force, we cultured T-cells at 37 °C for 30 min prior to cell fixation and staining. This is because TGT tension tolerance values for both the 12 and 56 pN probes were previously calculated at 37 °C (4). Moreover, the 12 and 56 pN TGT probes were selected based on the tension sensor results shown in Fig. 2A and E. The 56 pN probe is expected to provide the most mechanically stable tether, and thus remain hybridized to the surface resisting TCR forces that exceed ~19 pN. In contrast, the 12 pN TGT probes provide a labile tether that is expected to dissociate in response to TCR forces exceeding 12 pN. Thus, these two TGTs cap TCR forces at the most relevant critical thresholds of tension.

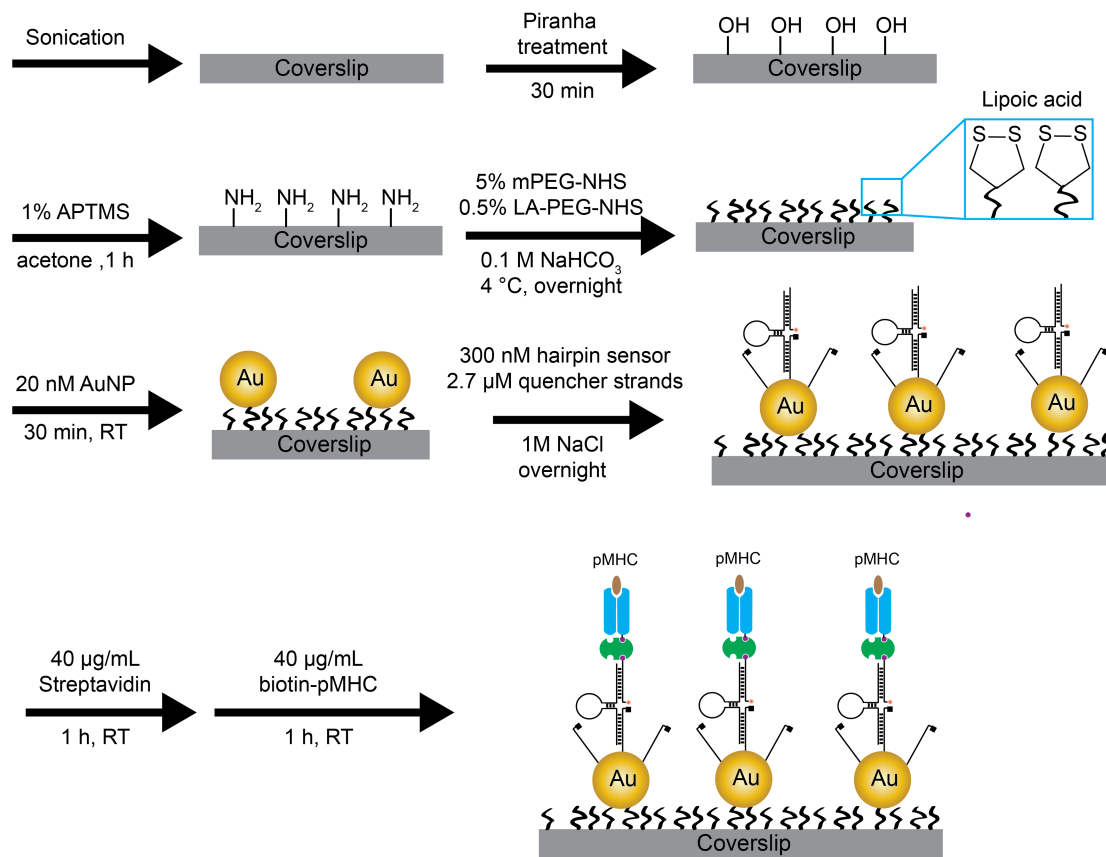


Fig. S1. Fabrication of DNA-based gold nanoparticle tension sensor surface. Flow chart showing the step-wise fabrication of DNA-based gold nanoparticle tension probes (see methods for full description).

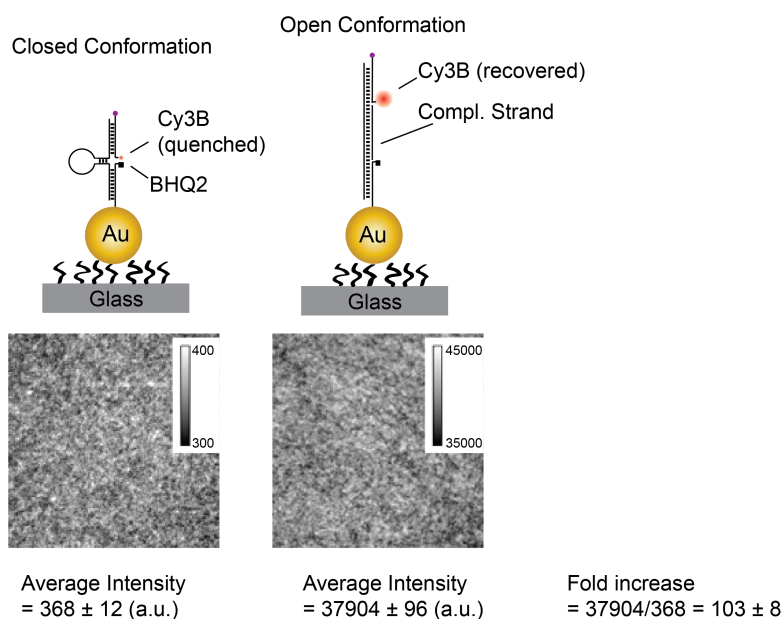


Fig. S2. Quenching efficiency calibration of DNA-AuNP tension probes. Scheme and representative images of the experiments used to determine the quenching efficiency of DNA tension probes on the AuNP surface. The closed conformation probe sample was prepared as described in the Fig. S1. The open conformation probe used a complementary strand to the scrambled hairpin at $0.3 \mu\text{M}$ (for sequences see Table 1 in methods section). This complementary strand generated a duplex, thus separating the dye from AuNP surface and the molecular quencher. This approach was adapted from energy transfer efficiency calibration experiments reported previously (5, 6). The calculated fold increase is 103 ± 8 .

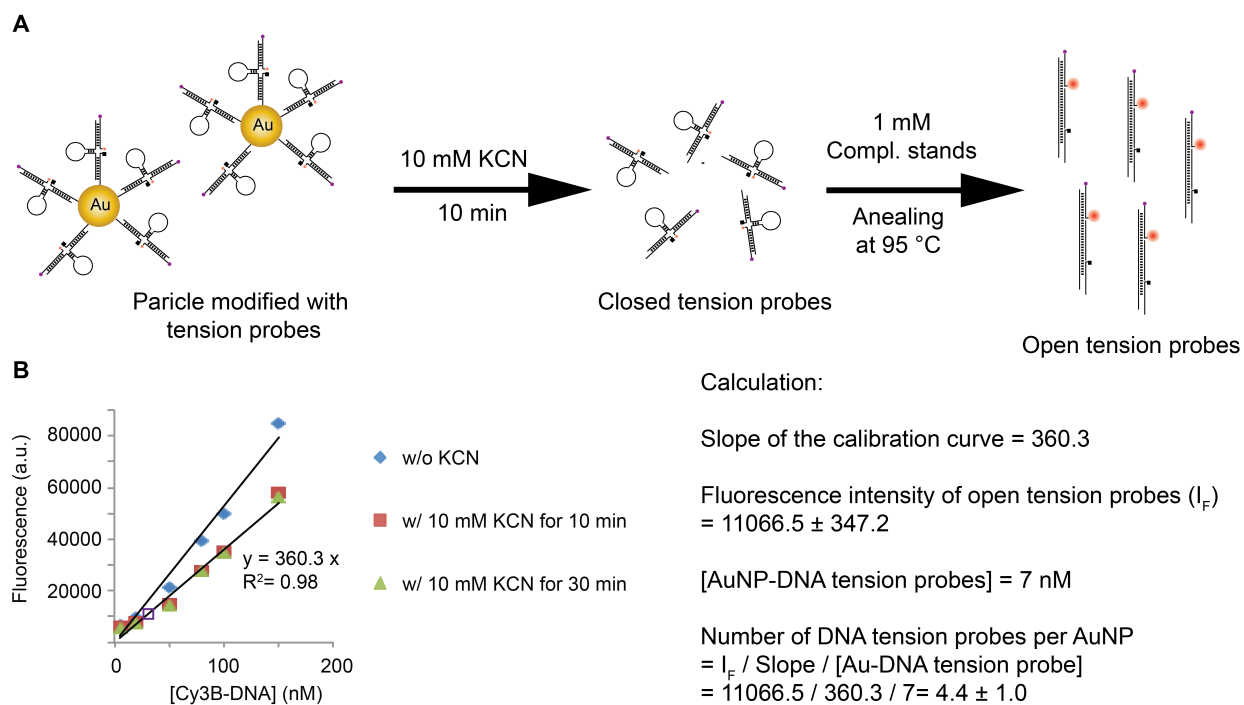


Fig. S3. Quantification of the average number of DNA sensors per gold nanoparticle. (A) Scheme showing the approach used to determine the average stoichiometry between Cy3B-labeled tension probes and AuNP. Briefly, the concentration of AuNP was determined from the absorbance at $\lambda=520$ nm. Subsequently, AuNPs were dissolved by treating the sample with 10 mM KCN, which released Cy3B-labeled tension probes within 10 min. 1 mM of complementary DNA was then added into the solution and heated up to 95°C for hybridization and opening of the hairpin. The fluorescence intensity of the released Cy3B dye was then used to determine the number of dye molecules in the sample. (B) Plots showing the calibration curve used to quantify the number of tension sensor ligands per AuNP. The blue diamonds represent the calibration curve for Cy3B without addition of KCN. The red squares and green triangles represent the calibration curve at different time points with KCN, while the purple box represents the sample containing the released Cy3B ligands from AuNP-tension probes. All measurements were performed in triplicate.

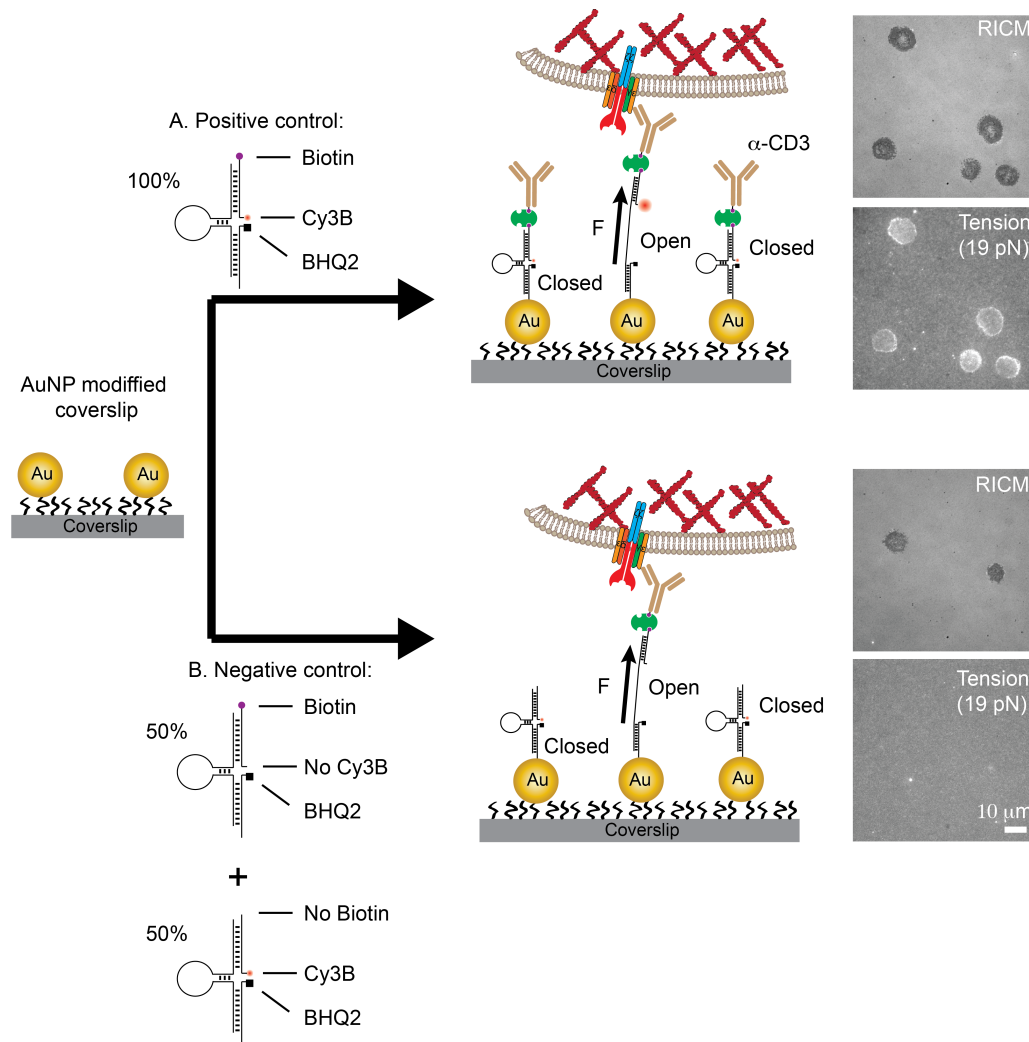


Fig. S4. Tension signals are specifically generated through TCR-ligand interactions. (A) Schematic representation of the procedure used to generate the positive control sample containing the DNA-based AuNP tension probes modified with α -CD3. The images show representative RICM and 19 pN tension signal for OT-1 cells cultured on the surface for 15 min. (B) Schematic representation of procedure used to generate the negative control sample which included AuNP modified with two types of hairpins at equal concentration. The first hairpin incorporated the Cy3B dye-BHQ2 quencher pair but lacked the biotin group at the terminus of the A21B strand. The second hairpin incorporated the biotin group but lacked the Cy3B dye on the A21B strand. Cell spread on these substrates. However, no detectable fluorescence signal was observed, showing that only specific interaction between TCR and its ligand leads to tension signal.

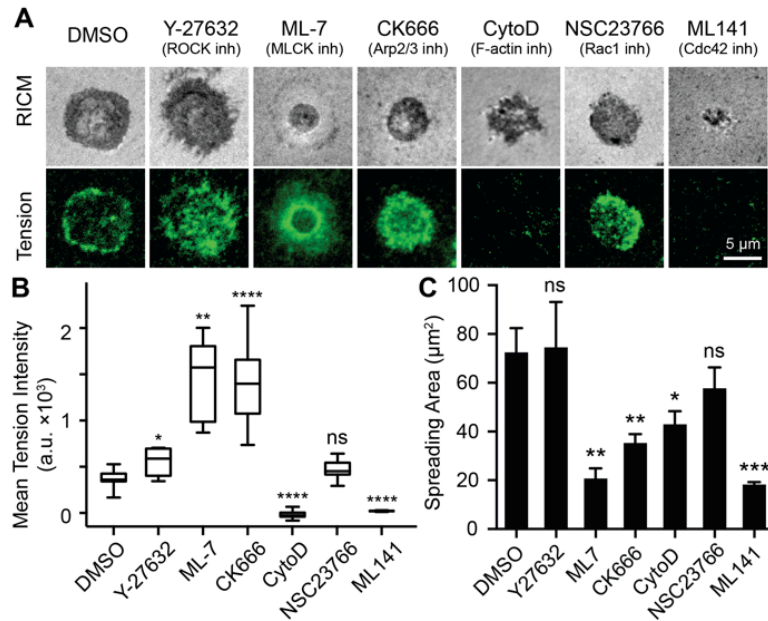


Fig. S5. Investigation of cytoskeletal elements mediating TCR forces. (A) Representative RICM and 19 pN TCR tension images of T cell treated with different cytoskeletal inhibitors. (B-C) Statistical analysis of 19 pN TCR tension (B) and cell spreading area (C) for T cells treated with different cytoskeletal inhibitors ($n = 20$ cells for each condition). All error bars represent s.d., * P -value < 0.1 ; ** $P < 0.01$; *** $P < 0.001$ and **** $P < 0.0001$.

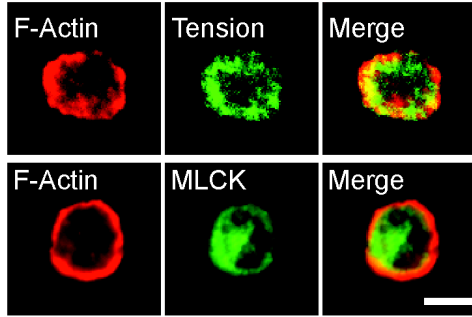


Fig. S6. Colocalization of TCR tension with F-actin, and F-actin colocalization with myosin light chain kinase. Representative immunostaining images of OT1 cells showing the colocalization between TCR tension (19 pN) and F-Actin assembly (top row) and F-actin colocalization with MLCK (bottom row). In general, F-actin and tension were highly colocalized, while we observed a spatial offset between the F-actin structure and the MLCK at the cell edge. Scale bar: 10 μm .

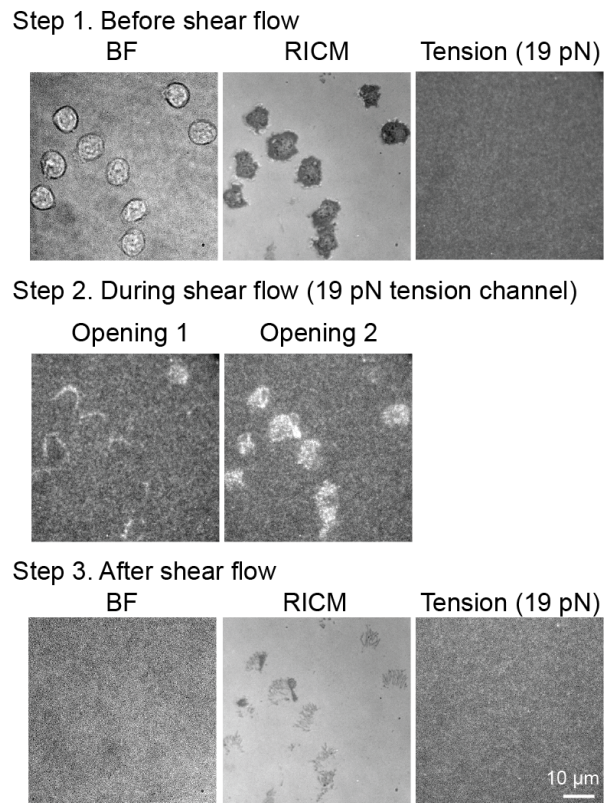


Fig. S7. Induction of 19 pN sensor by shear flow. Representative images showing that OT1 cells spread and generated no observable tension signals when they were plated onto the N4 decorated 19 pN tension probe surface (step 1). A strong shear flow was generated by pipetting a stream of imaging buffer into the cell chamber, which led to a step-wise increase in fluorescence intensity both at the edge and center (step 2). Eventually, the cells were removed from the surface (RICM) and tension probes recovered back to background levels (step 3).

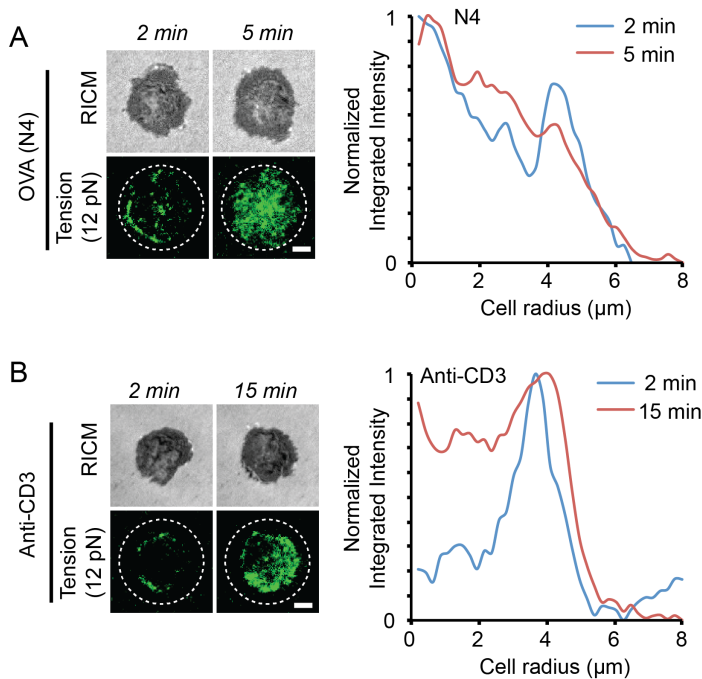


Fig. S8. Radial distribution function analysis of TCR tension upon ligand stimulation. (A) Representative RICM and 12 pN TCR tension images for OT-1 cells plated onto the N4 pMHC 2 and 5 min after cell-surface contact. The dotted circle represents the ROI used for radial distribution analysis using radial profile plugin in ImageJ. Plots show cell radius (r) vs fluorescence intensity for this cell at $t = 2$ min and 5 min following cell-surface contact. Analysis of tension at $t = 2$ min showed that forces were generally concentrated in a ring-like structure at the cell periphery. However, a peak at $t = 4-5$ min was observed in the central area. (B) Representative RICM and 12 pN TCR tension images for OT-1 cells plated onto the α -CD3 2 and 15 min after cell-surface contact. TCR tension at $t = 2$ min were concentrated in a ring-like structure. The characteristic ring-like structure was maintained for 15-60 min. Scale bar: 3 μm .

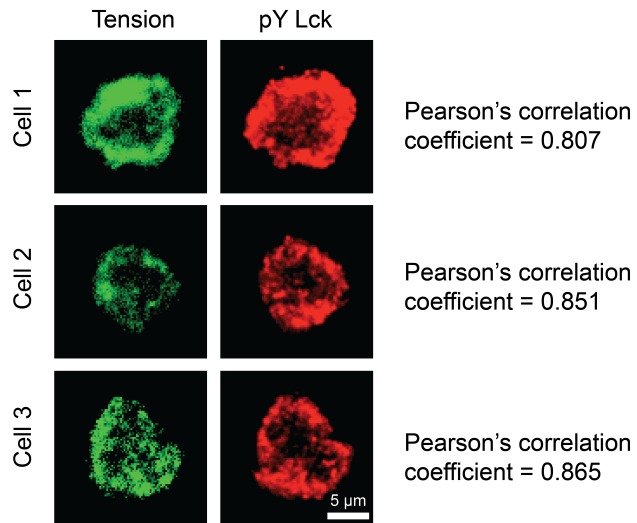


Fig. S9. Spatial correlation analysis between TCR tension and active Lck. Representative images of 19 pN TCR tension and phosphorylated Lck (pY394). Pearson's correlation coefficients were analyzed using the JACoP plugin implemented in Fiji. Briefly, individual cells acquired from each fluorescence channel were fed into the JACoP plugin, and the result of this analysis are reported here. $n = 20$ cells from 3 different chambers were analyzed and an average coefficient of 0.84 ± 0.04 was reported here.

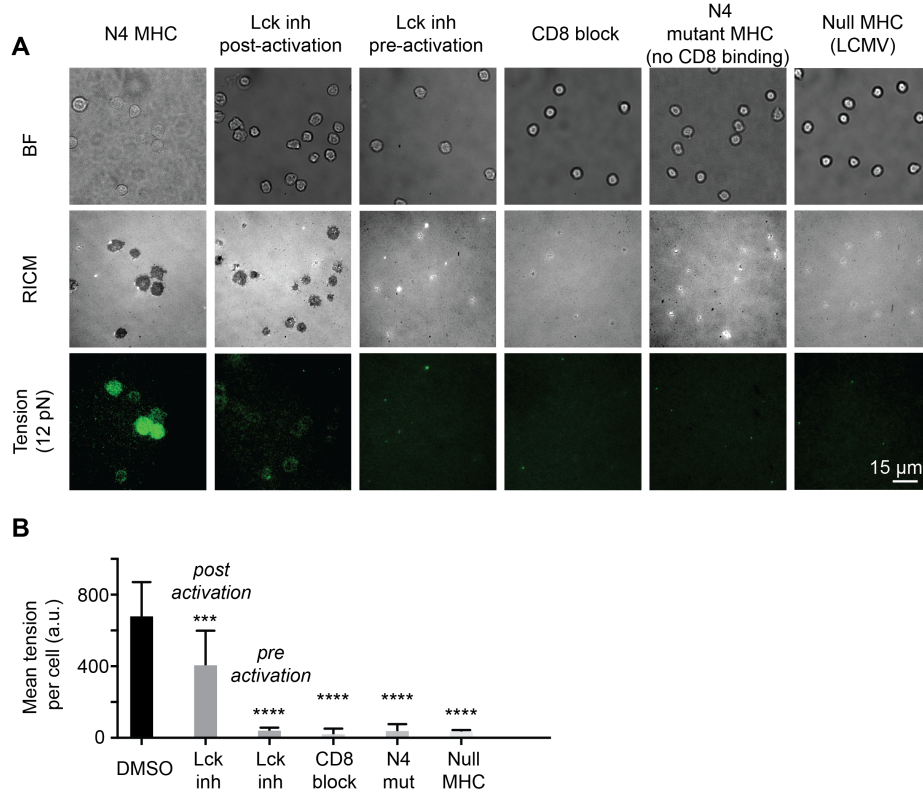


Fig. S10. Quantification of TCR tension upon perturbation of TCR, CD8 and Lck activities. (A) Representative brightfield, RICM and tension images showing differential T cell responses to different Lck inhibitors before (pre-activation) and after (post-activation) cell plating, CD8 blocking with antibody, mutant N4 pMHC with abolished CD8 binding, and null pMHC presenting the GP33-41 epitope from LCMV. (B) Bar graph quantifying the mean fluorescence tension signal per cell in responses to treatments described in (A). Error bars represent the standard deviation (S.D.) from $n = 20$ cells for each group. *** $P < 0.001$ and **** $P < 0.0001$.

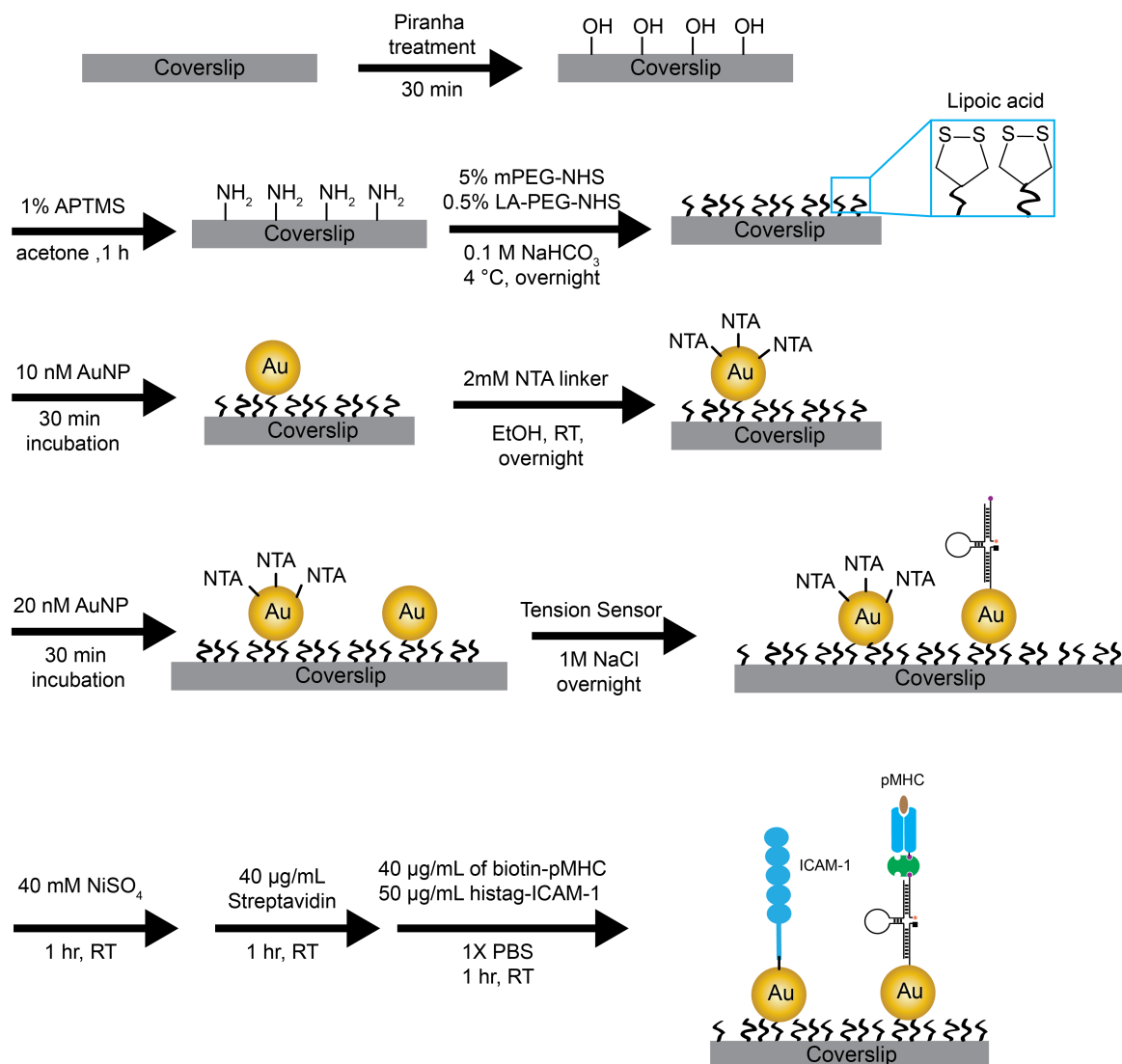


Fig. S11. Co-presentation of ICAM-1 and DNA tension sensor-pMHC ligands on AuNP. Flow chart showing the step-wise fabrication of AuNP surfaces co-presenting ICAM-1 and DNA tension sensor-pMHC ligands.

No.2 glass coverslips were rinsed and sonicated with nanopure water ($18.2 \text{ M}\Omega \text{ cm}^{-1}$) for 30 min, and then sonicated twice with acetone for 15 min. The slides were then dried in an oven set at 80°C for 10 min. Fresh piranha solution (7:3 v/v = H_2SO_4 : H_2O_2) was mixed and then used to clean the substrates for 30 min. Afterwards, the substrates were rinsed with a copious amount of nanopure water. The substrates were then sonicated in acetone to remove excess water and for further cleaning. Subsequently, 1% v/v APTMS solution in acetone was added to the slides and incubated for 2 h. The amine-modified coverslips were then rinsed in acetone and water and dried under stream of N_2 .

The slides were then annealed for 1 h at 80°C . The surface was then passivated with 5% w/v mPEG-NHS (MW 2000) and 0.5% w/v lipoic acid-PEG (MW 3400) in 200 μl of 0.1 M fresh

sodium bicarbonate solution. After overnight incubation at 4 °C, the excess unreacted PEG molecules were rinsed with nanopure water. This strategy affords a glass surface with sufficient lipoic acid groups to irreversibly anchor AuNP MTFM sensors at appropriate densities. Next, 10 nM of unmodified 9 nm AuNP solution was incubated for 30 min and then rinsed with nanopure water to remove nonspecifically bound particles.

400 µl of 2 mM of NTA-SAM reagent in pure ethanol was incubated with the AuNP modified coverslips overnight at RT. The coverslips were then placed in a petri dish containing pure ethanol to prevent sample from drying. After rinsing with copious ethanol, the coverslips were air-dried and incubated with 40 mM of NiSO₄ solution for 1 h. Afterwards, an additional 20 nM solution of unmodified AuNPs was incubated with the coverslip for 30 min before modification of tension probes.

The DNA tension probe hairpins were assembled in 1X PBS by mixing the Cy3B labeled A21B strand (0.33 µM), quencher strand (0.33 µM) and hairpin strand (0.3 µM) in the ratio of 1.1: 1.1: 1. The solution was then heated to 95 °C for 5 min by using a heat block and cooled back to room-temperature over a period of 30 min. Afterwards, an additional 2.7 µM of BHQ2 strands were introduced into the DNA assembly solution in 1 M NaCl. 100 µl of this final solution was added between two AuNP functionalized coverslips and incubated overnight at 4°C.

DNA tension probe modified coverslips were rinsed in 1X PBS before further functionalization with 40 µg/ml of streptavidin in 1X PBS. After 1 h incubation, the coverslips were rinsed in 1 X PBS to remove the unbound streptavidin, which was followed by the final modification with a mixture of 40 µg/ml of biotinylated ligands (pMHC or α-CD3) and 50 µg/ml of histag-ICAM-1 in 1X PBS for 1 h.

These modified coverslips were then assembled into cell imaging chambers (Attofluor, Life Technologies) filled with hank's balanced salt imaging buffer and immediately used for cell experiments.

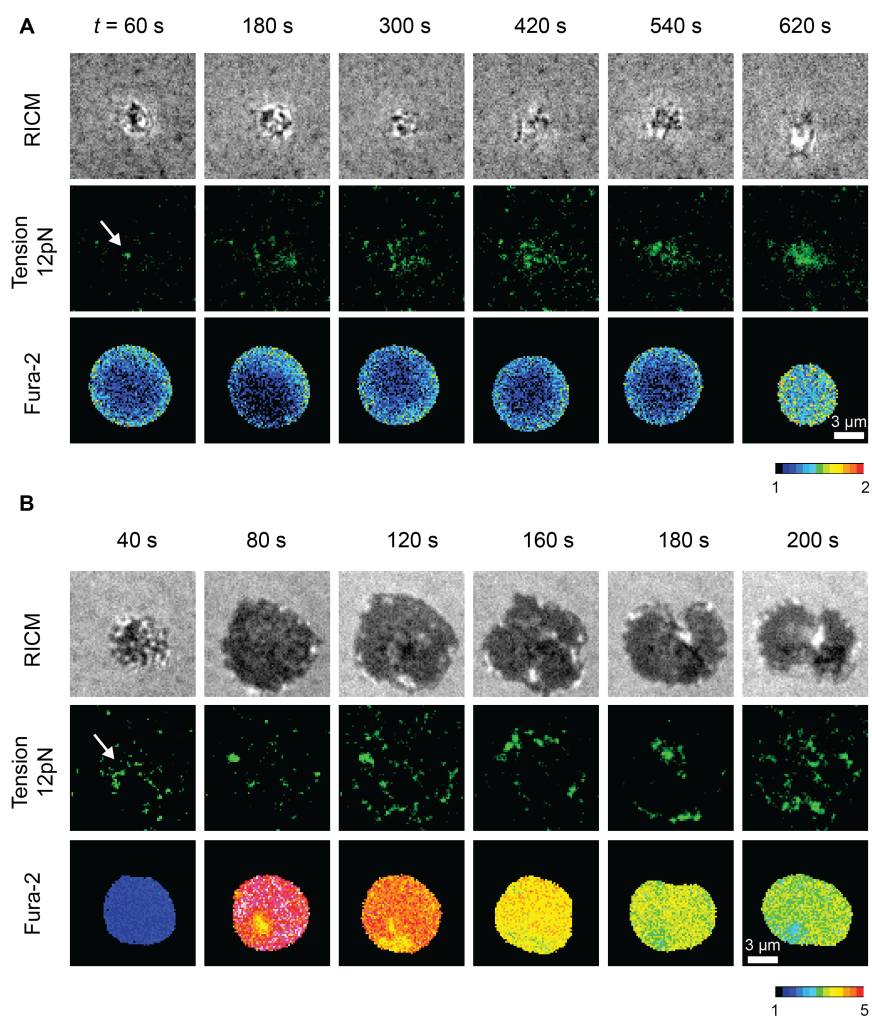


Fig. S12. Comparison of TCR forces and calcium flux between V4 and N4 ligand. Simultaneous imaging of cell spreading (Reflection interference contrast microscopy, RICM), 12 pN TCR forces (tension) and T cell activation (fura-2) for a representative OT-1 cell encountering V4 pMHC (A) and N4 pMHC (B). White arrow indicates the initial appearance of tension signals within 1 min of cell-substrate contact.

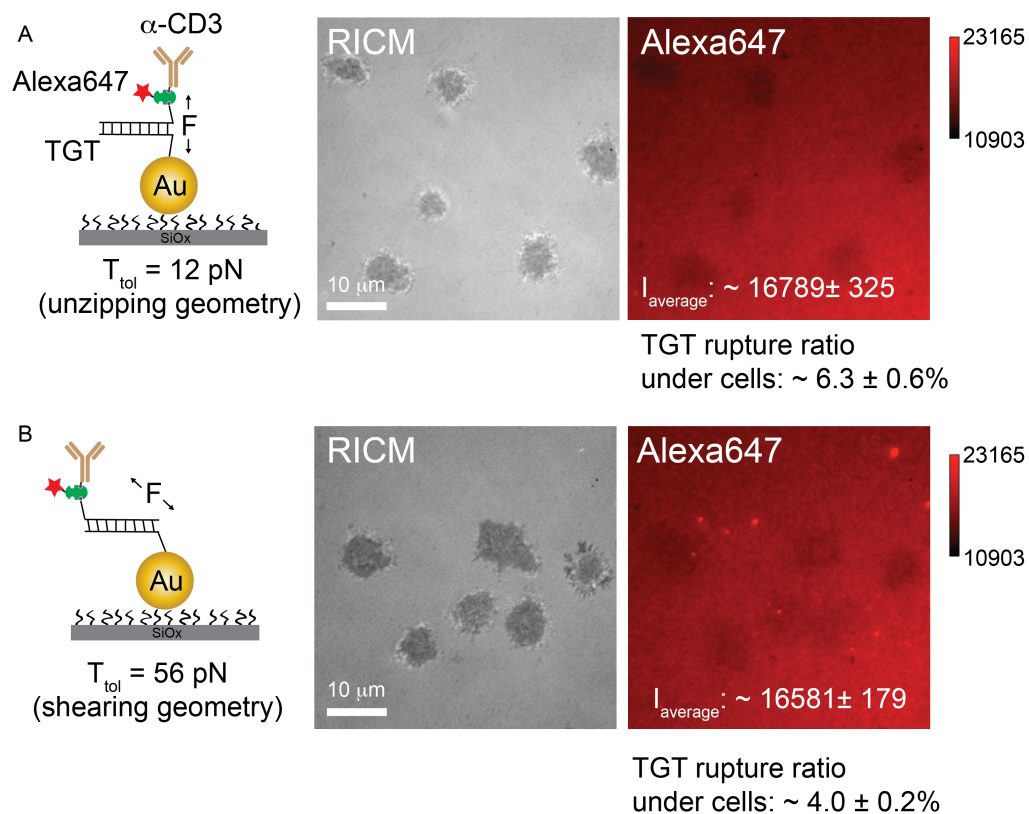


Fig. S13. Comparison of TGT rupturing between 12 pN and 56 pN probes. (A) Schematic representation of 12 pN TGT modified with α -CD3. RICM and fluorescence images show the result of T cells cultured on this surface for 30 min. T cells spread and generated mechanical forces that dissociate the TGT duplex, leaving an area with decreased fluorescence intensity. Quantification analysis showed a $6.3 \pm 0.6\%$ decrease in fluorescence due to DNA rupturing. (B) Schematic representation of 56 pN TGT modified with α -CD3. Upon plating, OT1 cells spread and generated mechanical forces that reduced the streptavidin intensity by $4.0 \pm 0.2\%$. These results confirmed the model that 56 pN TGT provided greater mechanical resistance than the 12 pN TGT. $n = 20$ cells were analyzed.

References

1. Woodside MT, *et al.* (2006) Nanomechanical measurements of the sequence-dependent folding landscapes of single nucleic acid hairpins. *Proc Natl Acad Sci USA* 103(16):6190-6195.
2. Blakely BL, *et al.* (2014) A DNA-based molecular probe for optically reporting cellular traction forces. *Nat Methods* 11:1229-1232.
3. Yokosuka T, *et al.* (2005) Newly generated T cell receptor microclusters initiate and sustain T cell activation by recruitment of Zap70 and SLP-76. *Nat Immunol* 6(12):1253-1262.
4. Wang XF & Ha T (2013) Defining Single Molecular Forces Required to Activate Integrin and Notch Signaling. *Science* 340(6135):991-994.
5. Liu Y, Yehl K, Narui Y, & Salaita K (2013) Tension Sensing Nanoparticles for Mechano-Imaging at the Living/Nonliving Interface. *J Am Chem Soc* 135(14):5320-5323.
6. Jennings T, Singh M, & Strouse G (2006) Fluorescent lifetime quenching near $d = 1.5 \text{ nm}$ gold nanoparticles: probing NSET validity. *J Am Chem Soc* 128(16):5462-5467.